Dose and Microdose Measurement based on Threshold Shifts in MOSFET arrays in Commercial SRAMS

Leif Scheick and Gary Swift

ABSTRACT **A new dosimetry method using an array of MOS transistors is described for measuring dose absorbed from ionizing radiation. The method uses direct measurement of the number of cells that change state as a function of applied operating bias to a SRAM as a function of absorbed dose. Since the input and output of a SRAM are digital, the measurement of dose is easily accessible by a remote processing system. The devices show minimal response to total ionizing dose, but individual SRAM cells show strong micro-dose effects.**

I. INTRODUCTION

Electron-hole pairs are generated in all areas of a device when ionizing radiation interacts with microelectronics [1]. Some of these electrons and holes are bound in the various oxides of the structures that comprise an integrated circuit. A particularly susceptible device is the MOSFET, or more specifically the oxide between the gate and the channel. In fact, the RADFET dosimeter is based on a p-channel MOSFET specifically designed to maximize the change in threshold voltage of the transistor as a function of radiation.

The memory cell of a CMOS SRAM contains six MOSFETS. Two p-channel and two n-channel devices comprise a CMOS SRAM cell. Two n-channel access transistors isolate the cell from the rest of the device. Each of these has a shift in threshold voltage with radiation as with regular MOSFETs. Due to this shift in transistor threshold, the voltage at which the SRAM cell cannot be read or cannot hold its logic state should depend on the dose applied. Each cell should exhibit this response on the microvolume scale as well, therefore causing each cell on the device to yield independent microdose measurements for a heavy ion that strikes a sensitive volume. The sensitive volume in the cell is the gate oxide of the transistors that make up the SRAM cell.

MOSFETs have been studied in depth for dosimetry and microdosimetry applications [2], [3]. These studies show that both discreet and continuous radiation fields can be measured by single MOSFET based dosimeters. SRAMs have been studied extensively for TID and SEE behavior [4]-[16]. From these studies, the following facts are common in SRAM radiation response. SRAMs have differing sensitivities to radiation when different biases are applied during irradiation [4]-[6], [10]. SRAM cells, under certain circumstances, can retain effects of dose on individual cells [6], [8], [9]. The radiation response should mostly be due to interface traps, since the bulk traps in thin gate oxides used in IC CMOS fabrication will not make a dominant contribution to MOSFET threshold response [1], [7], [10].

[1] Manuscript received July 16, 2002. The research in this paper was carried out by the Jet Propulsion Laboratory, California Institute of Technology under contract with the National Aeronautics and Space Administration (NASA) Code AE, under the Electronic Parts and Packaging Program (NEPP).
L. Sscheick and G. Swift are with the Jet Propulsion Laboratory, California Institute of Technology, Pasadena, CA 91109 USA (telephone: 818-354-3272, e-mail: leif.scheick@jpl.nasa.gov).

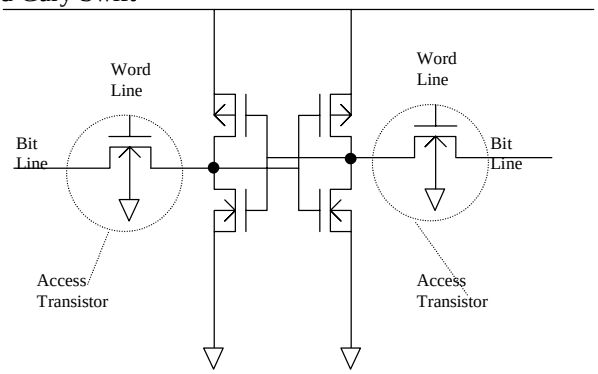

Fig. 1. A CMOS SRAM cell. The threshold shift in the transistors should be sufficiently sensitive to dose to cause readout changes at different operating biases.

The SRAM based dosimeter will have several innovative properties. The device will accrue dose in a stand-by bias, which is due to inherent stability in the SRAM cell. The device will use low power. Heavy ion hits on SRAM sensitive volumes (SV) will cause the hit SRAM cell to show a large response in the voltage at which a cell cannot hold its logic state. The programming and reading of the device is digital.

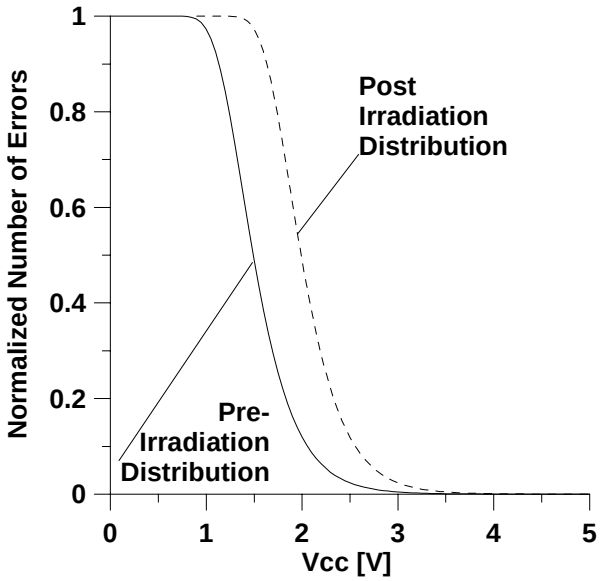

Fig. 2. The hypothetical fraction of cells to report an error (0 to 1) as a function of the bias at which the device is readout. The device will be programmed at normal operating bias and then readout at a reduced operating bias. The dotted curve shows a possible response to radiation. The overall shift of the distribution would be calibrated to measure dose.

II. THEORY

The SRAM cell uses two CMOS inverters to lock a logic value into one another. A simple SRAM cell is shown in Fig.1. The value of the cell is changed by turning on the access transistors, near the bit line, and pulsing in a new value. Reading is essentially the same, except that the access

transistors are activated, and sense amplifiers read out the state of the outputs of the inverters.

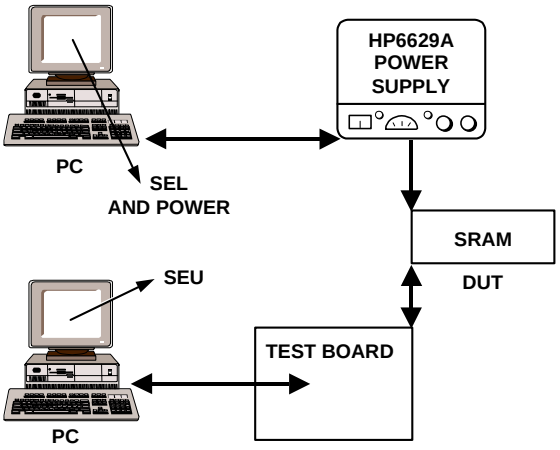

Fig.3. A block diagram of the test system.

SRAM based dose measurement is made possible by the properties of the four MOSFETs that make up the SRAM bit. A CMOS inverter consists of a p-channel and an n-channel MOSFET with the gates tied together (input) and the drains tied together (output). The source of the pmos transistor is connected to Vcc, while the source of the nmos transistor is grounded. The n-channel will exhibit a negative threshold shift, due to positive charge in the bulk oxide, and then rebound toward a positive voltage shift due to interface traps. The extent of the rebound depends on transistor manufacturing parameters, dose rate, temperature, and other factors. The p-channel device accrues both bulk and interface charge of positive polarity, so its shift will always be in the negative direction. For this reason, RADFETs are p-channel devices.

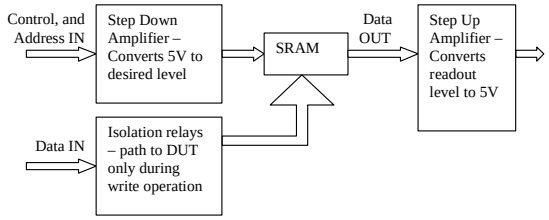

Fig.4. A conceptual diagram of the test board that allows variable biasing of the device.

Unlike discrete MOSFETs, the MOSFETs that make up a SRAM cell do not have a thick oxide. Positive bulk trapping, therefore, should not be a dominant issue. The interface threshold shifts should be the main radiation effect. This effect may keep the SRAM cell fairly robust in terms of holding the memory state at the same threshold after irradiation. The response to equally irradiating all four SRAM cell transistors should result in a symmetrical response, i.e., the nmos will have a positive shift and the pmos will have a negative shift. Irradiating the whole cell uniformly should not result in a large change in the bias at which the SRAM cell cannot hold its programmed value. Thin oxides, also, indicate that the voltage shift resulting from trapped charge will be minimal [1].

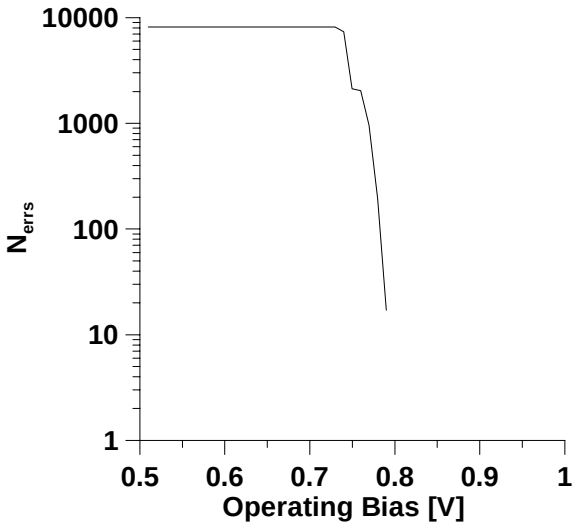

Fig. 5a. The number of cells to report an error (0 to 1) as a function of the readout bias. This device is a Toshiba SRAM.

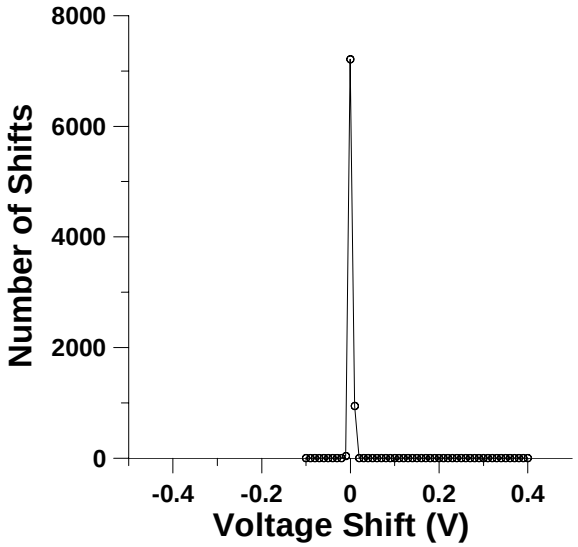

Fig. 5b. A histogram of shifts in threshold voltage (0 to 1) as a function of the readout bias. The device is the Toshiba SRAM. Other devices have similar response with slightly wider distributions. More than 99% of the cells report an error within 0.01 volts of the value at the bit from a previous readout.

If a high dose is deposited to one of the gate oxides from a single ion strike, then the struck transistor should experience a high local dose and exhibit a large threshold voltage shift. If only one of the transistors experiences a threshold shift, the voltage at which the SRAM cannot hold the programmed value will change, as the inverters are no longer symmetrical. Therefore, a cell may have a minimal TID response, but a strong microdose effect. The implication, then, is that the SRAM should be a heavy ion microdosimeter but also an insensitive total dose dosimeter.

Microdose is related to stuck bits, or single hard errors (SHE), in SRAMs and other memories. Studies have been conducted concerning this phenomenon [8], [12], [14]. The microdose response in this study of single event shifts should be described by the same analysis as has been

employed in studying SHE. A SRAM cell that fails to hold its programmed state at higher bias before irradiation by a heavy ion is equivalent to a latent stuck bit observed in other SRAM studies [8].

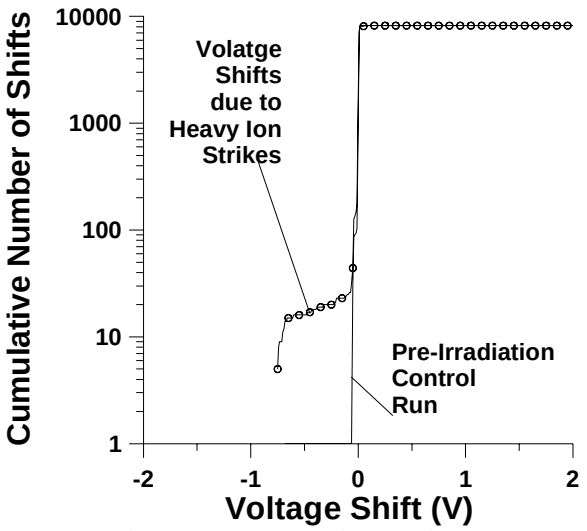

Fig. 6. Depiction of the graphical method of analysis for microdose response of the devices. The figure shows the cumulative shifts from ion-induced shifts for a control curve (solid line) and a curve with some radiation induced shifts (dots).

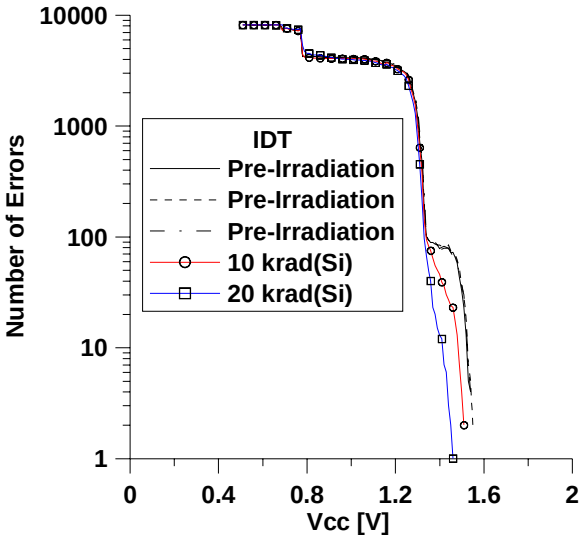

Fig. 7a. The number of cells to report an error (0 to 1) as a function of the readout bias as a function of dose for an IDT part. Approximately one percent of the cells show errors at higher voltages. This effect is too small for a dosimetry application and is most likely due to increased noise in the CMOS readout circuitry.

The technique used to employ a SRAM as a dosimeter begins with programming the device as with normal operation. The bias on the Vcc and all input pins on the SRAM is ramped down and read. As the bias decreases, there should be a change in the number of cells that cannot maintain the programmed state. A hypothetical curve that plots the fraction of cell failures as a function of bias is shown in Fig. 2. The total dose response should be a shift of the distribution to a higher or lower voltage at which half the cells have errors. Micro-dose effects should drive cells hit by an ion to exhibit threshold shifts that are well outside of the post-irradiation distribution. The technique used in this study leverages from techniques successfully used in previous studies [16]-[18].

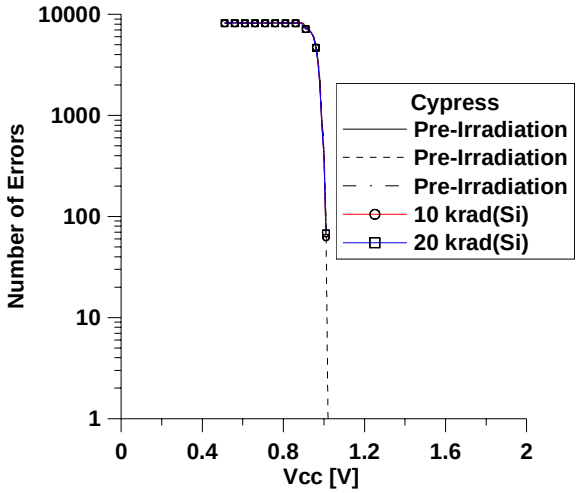

Fig. 7b. The number of cells to report an error (0 to 1) as a function of the readout bias as a function of dose for a Cypress part. The device shows no overall TID effect.

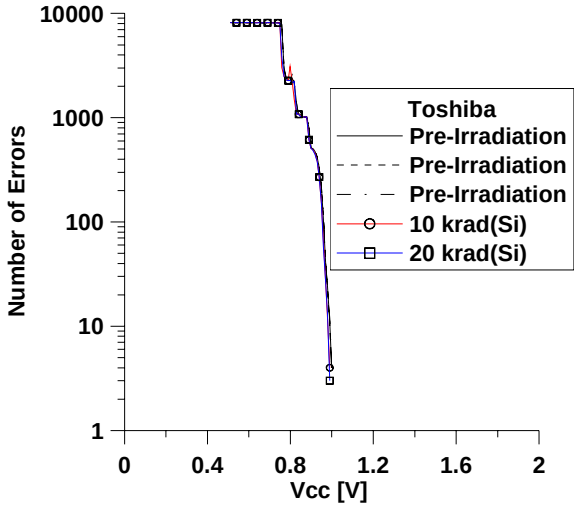

Fig. 7c. The number of cells to report an error (0 to 1) as a function of the readout bias as a function of dose for a Toshiba part. The device shows no overall TID effect.

Shifts to lower voltages were neglected for this study and will be addressed in later studies. This approach was chosen for three reasons. A shift in the threshold voltage for a single transistor in a SRAM cell will shift the voltage at which a SRAM will not hold its programmed state higher. This effect is a general property of an asymmetrical SRAM cell [19]. Previous studies have shown that SRAMs work at low voltages, between 2 and 0.7 volts [8]. It is more feasible, therefore, to measure the shift to higher voltage since an SRAM will have more range to show the response. Finally, a voltage shift to less then 0.7 volts is unreliable as this is below the 0.7 volts that the pn junction of a forward biased drain requires to remain properly activated. So, shifts to lower voltages are untenable for this study, and are neglected.

TABLE I.
DEVICES USED IN THIS STUDY.

Device	Mfg.	Dev ID	Date Code	Alt Code
CMOS SRAM	Cypress	CY62128VLL-70SC	0147PHI	641642
CMOS SRAM	Toshiba	TC554001AF-70L	01514MAD	Y71247
CMOS SRAM	IDT	IDT71024	M0207M	S12TY
CMOS SRAM	ISS	IS61C1024-15KI	0144	JW380631 S4

TABLE II.
AVERAGE NUMBER OF HITS TO A SRAM CELL

Fluence [cm^{-2}]	Ave num hits per SRAM cell
1.20E+07	1.17
4.80E+07	4.69
9.60E+07	9.38
1.96E+08	19.1

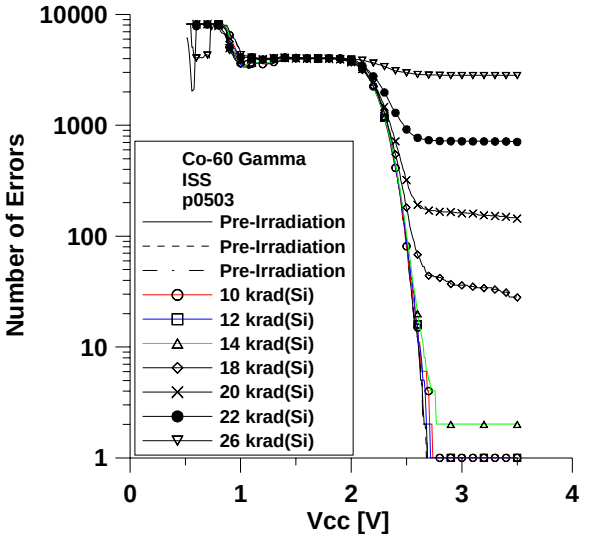

Fig. 7d. The number of cells to report an error (0 to 1) as a function of the readout bias as a function of dose for an ISS part. The device shows a fairly strong TID effect but is not reproducible from part to part. This response may be due to the peripheral circuitry and is not applicable to dosimetry.

III. EXPERIMENTAL PROCEDURE AND SETUP

The test equipment was comprised of two PCs, a power supply, and a specially designed test board. One PC controlled a HP6629A power supply. This configuration allowed precision voltage control and latch-up detection and protection, since the PC had millisecond control over the operation of the power supply. A dedicated PC controlled the test circuit board designed specifically for this SRAM test to read and write to the DUTs. This setup allows complete freedom to interact with the DUT. The address of a failure and the value at that address were recorded in a file for each run, allowing for any structure in the SEEs or predilection for certain failure patterns or types of SEU to be observed. A depiction of the setup used is shown in Fig. 3. The Vcc voltage was always set to 5 volts for writing and irradiation. The device was in read mode for all irradiations. The operating temperature was approximately 25°C throughout the study.

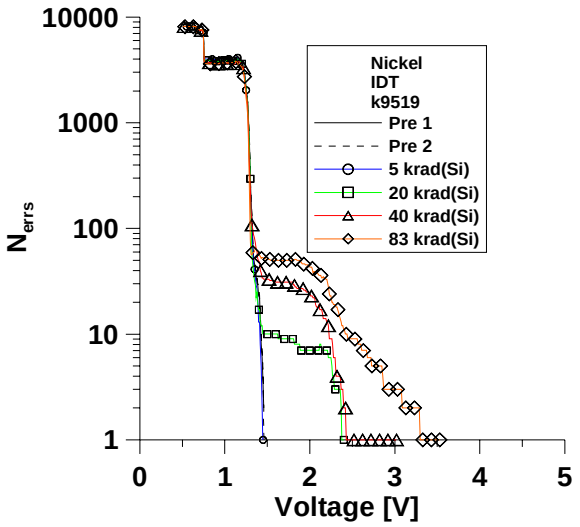

Fig. 8. Total overall dose response to a DUT to heavy ions. Many of the cell effects are buried in the distribution so the method outlined in Fig. 6 will show this effect more clearly.

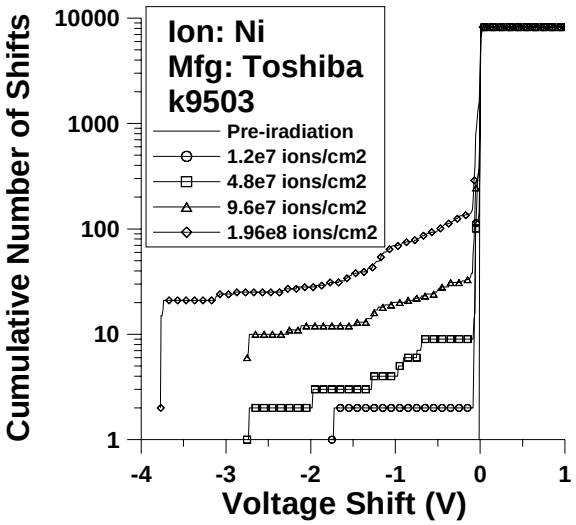

Fig. 9a. Cumulative distributions of threshold voltage shifts for increasing fluences by nickel on a Toshiba SRAM.

The protocol for the experiment is as follows. Each device is programmed with a zero value at each bit location. 8192 bits are readout while ramping down the bias on the Vcc and input pins. 8192 bits were chosen as a sufficiently large statistical sample to allow for readout celerity during experiments at the beam site. Pre-irradiation runs are conducted to determine the pre-irradiation curve, and the voltage at which each bit reports an error is recorded. After the biased device is irradiated while standing by in read mode, the device is programmed at 5V, and the voltage is then ramped down and read. The metric is the number of cells that could not report the programmed state at each bias level.

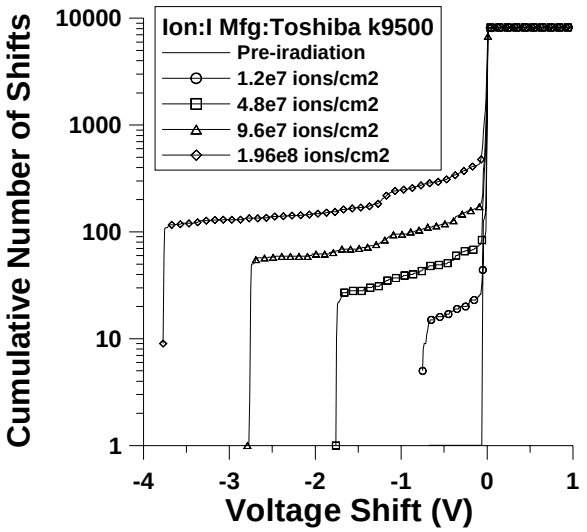

Fig. 9b. Cumulative distributions of threshold voltage shifts for increasing fluences by iodine on a Toshiba SRAM. The equal steps of largest shifts are an artifact of the measurement technique. The experimental protocol for this run underestimated the shifts that iodine would induce and so certain bits show events at the largest sampled voltage.

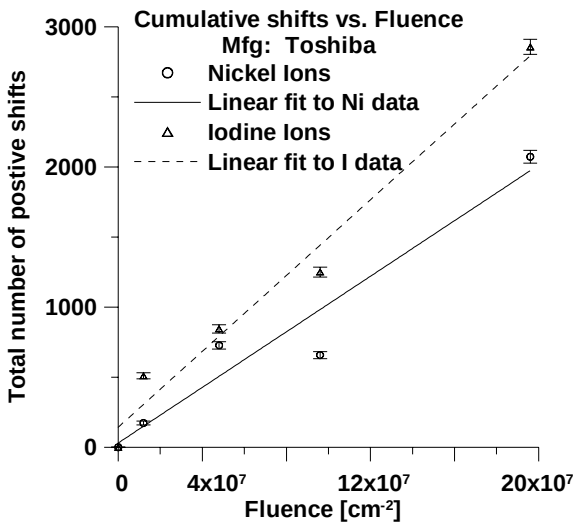

Fig. 9c. Total number of positively shifted SRAM cells as a function of ion fluence. The error bars are based on Poisson counting statistics.

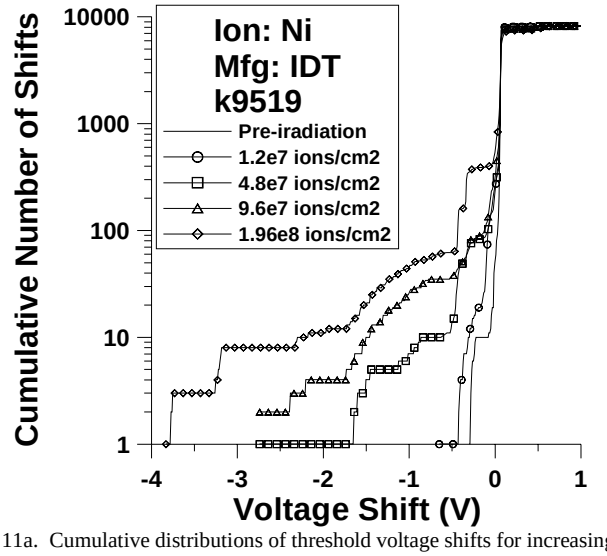

Fig. 11a. Cumulative distributions of threshold voltage shifts for increasing fluences by nickel on an IDT SRAM.

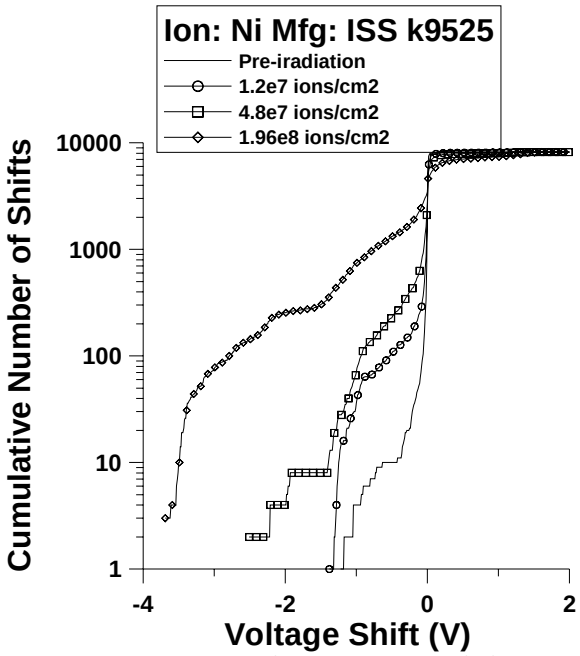

Fig. 10a. Cumulative distributions of threshold voltage shifts for increasing fluences by nickel on an ISS SRAM. The pre-irradiation curve, the solid line, has considerable noise, but still shows a strong microdose effect.

A flight application of this dosimeter would follow the design shown in Fig. 4. A DAC would select a reduced bias for the SRAM and a voltage step-down/step-up converter to supply to I/O pins of the SRAM. This dosimeter would require 10 to 20 SOIC chips that could be accessed directly from a bus. The current would be minimal, in the mA range, since CMOS devices would be used.

Listed in Table I, Four different SRAMs were analyzed using the aforementioned approach. Since manufacturing variances have been shown to greatly affect radiation sensitivity and device performance in IC-based dosimeters [7], [11], [13], [17], [19], a variety of devices were chosen to examine the variance. This practice allows the variables of production and design to be observed in dosimeter response.

Total dose irradiations were conducted at the cobalt-60 facility at JPL. All cobalt-60 irradiations were done at a dose rate of 25 rad/s. The Co-60 source used to irradiate these devices presents a continuous radiation field to the part. Each transistor in the SRAM cell, therefore, will be equally dosed. Since the test devices are all COTS CMOS devices, the total dose limit of the peripheral circuitry limits the dynamic range of this device. The issue of the hardness of the SRAM sense amplifiers kept the total dose under 20 krad(Si) for gamma dose. Since the dose from heavy ions is highly localized, the upper limit was set to 100 krad(Si). The supply current was monitored during exposure to ensure that the current stayed within specifications.

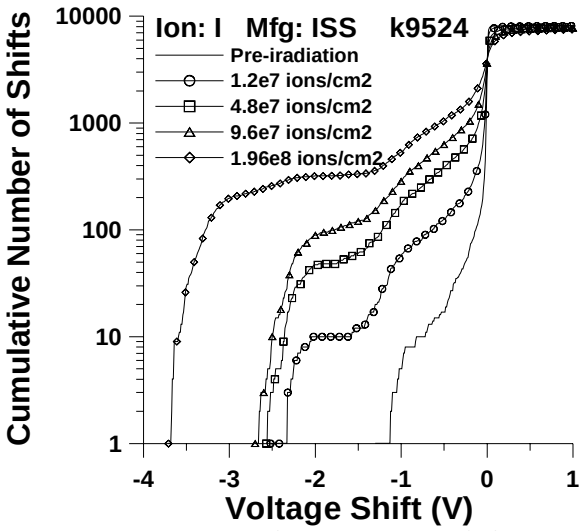

Fig. 10b. Cumulative distributions of threshold voltage shifts for increasing fluences by iodine on an ISS SRAM.

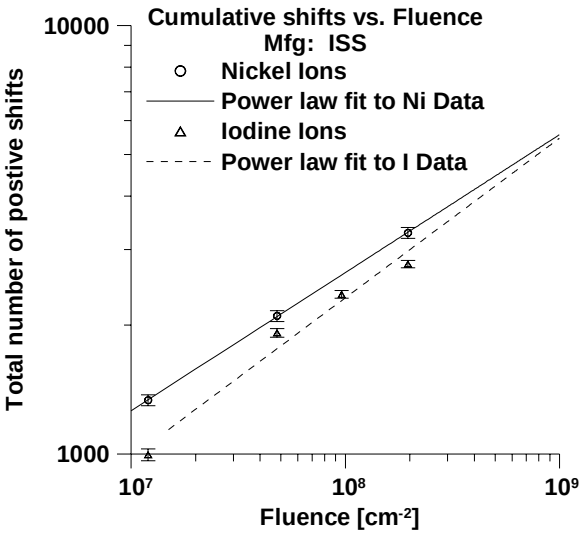

Fig. 10c. Total number of positively shifted SRAM cells as a function of ion fluence. Both ions have statistically similar power law behavior. The error bars are derived from Poisson statistics.

Heavy ion irradiations were conducted at the SEE line at Brookhaven National Laboratory. When the device was irradiated with heavy ions, the following cumulative fluences were chosen: 1.2e7 cm^{-2}, 4.8e7 cm^{-2}, 9.6e7 cm^{-2} and 1.96e8 cm^{-2}. These fluences were chosen so that each SRAM cell would be hit once on average for 1.2e7 cm^{-2} fluence to several times, on average, for the highest fluence. The actual sensitive volume is much less than the area of a cell. Table II lists the average number of hits to a cell. The dose for heavy ions at these fluences is very localized.

A. Device Characteristics

1) Macro Response

A typical pre-irradiation readout data set is shown in Fig. 5 for a Toshiba part. The other three devices have similar pre-irradiation curves, and discontinuities similar to those seen in Fig. 5a are typical. The narrow distribution implies processing and manufacturing variations in circuit elements do not contribute to noise. An applicable response will be a shift of the distribution such as the distribution hypothesized in Fig. 2. Any repeatable and measurable shift can be calibrated for a dosimetry application.

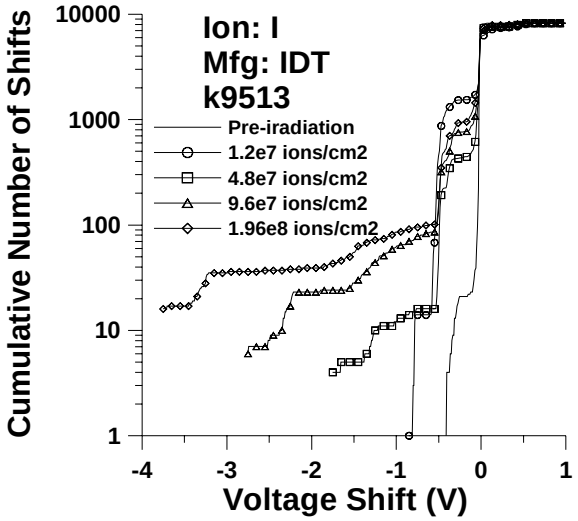

Fig. 11b. Cumulative distributions of threshold voltage shifts for increasing fluences by iodine on an IDT SRAM.

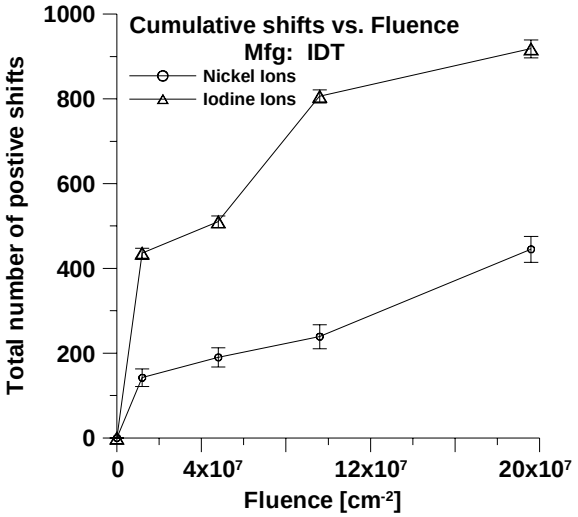

Fig. 11c Total number of positively shifted SRAM cells as a function of ion fluence.

2) Micro Response

Fig. 5b is the distribution of shifts in the threshold voltage at which a SRAM cell reports an error for two identical runs. Since the threshold shift is defined as the pre-irradiation threshold minus the post-irradiation threshold, it is negative when a cell reports an error at a higher voltage and is the metric under study. As seen in the figure, the threshold voltage is very precise and these devices are very repeatable in terms of voltage shift for each cell. Therefore, any threshold shift due to radiation should be observed.

Heavy ion irradiation is expected to cause single SRAM cells to exhibit large threshold shifts. This effect is very similar to single hard errors observed in previous studies [8]. This response may not be obvious in the raw distribution. To see this response more clearly, each cell's threshold

voltage is compared before and after irradiation, which is shown graphically in Fig. 5b. Plotting the integral distribution of the threshold shift clearly shows the effect, which is depicted graphically in Fig. 6.

IV. RESULTS

A. Total Dose Results

The result of each type of device having been irradiated to 20 krad(Si) is shown in Fig. 7. The Toshiba, IDT, and Cypress parts do not exhibit a strong or predictable response to overall gamma TID, which was predicted if the gate oxides were thin. The Cypress and Toshiba parts, Fig. 7b and 7c respectively, show no response to dose. The IDT part, Fig. 7a, shows a small amount noise related effect at the highest readout voltages, but is not repeatable or applicable to total dose dosimetry. The Toshiba, Cypress, IDT and ISS devices would not make effective total dose dosimeters.

The ISS part exhibits an erratic total dose response. This part shows errors after 10 krad(Si), but not in a repeatable way. It is not clear that this effect is not failure of the peripheral circuitry. The ISS results were not consistent from part to part within the experimental lot, which further intimates that the peripheral circuitry is soft to total dose.

All devices exhibit parametric failure after 20 krad(Si), due to increased supply current. Future applications of these devices will require countermeasures to the total dose weakness of the peripheral circuitry, such as passive irradiation, segregated dosing of the array, or hardened design only of the peripheral circuitry. Other modes of irradiation, shielding, and readout will be investigated to increase robustness and sensitivity in later works.

B. Heavy Ion Results

Virgin devices were irradiated by two different heavy ions. They were nickel (LET = 26.6 MeV/mg/cm^2) and iodine (LET = 60 MeV/mg/cm^2). These LETs were chosen to cause a large effect on the cells, but still vary the LET by a factor of two. The supply current was monitored for parametric failure, and the devices were observed to maintain current within specifications. Some devices were delidded in such a manner as to expose only the SRAM array to the ions but not to peripheral circuitry. No difference in device operation was observed between the fully delidded and partially delidded parts.

1) Heavy Ion Total Dose

The total number of errors for an IDT part as a function of Vcc voltage for nickel radiation is plotted in Fig. 8. The difference from the Co-60 total dose response is that there are errors at higher bias not present in the gamma dose experiment, Fig. 7a. These events are attributed to rare energy depositions by heavy ions in a sensitive volume. There was, however, no overall shift in the distribution from an overall dose, which agrees with total dose response from gamma radiation.

The Cypress part exhibited no total dose response to heavy ions, with no outliers. This part showed outstanding radiation robustness both on the macro and micro scales. Future study to optimize these devices for sensitivity will examine this effect in depth. The property that makes the Cypress device a robust dosimeter can be capitalized on to increase sensitivity in later designs. The total number of shifts observed was small in magnitude, there were none in excess of 0.01V, but the amount slightly increased with fluence.

2) SRAM Cell Heavy Ion Effects

Fig. 8 demonstrates that, while the overall total dose response in negligible, there are many cells that report error voltage outside of the post irradiation distribution. This effect was not observed in the gamma radiation response. The phenomenon is a microdose effect, and it can be more easily studied by using the graphical analysis method shown in Fig. 6. By plotting the distribution of threshold shifts from heavy ions, the effect on the cell level can be more easily determined. To better illustrate the effect of the ion, the distributions are plotted in integral form. This technique is performed by integrating the number of cells for each voltage shift from negative voltage to positive voltage. Figures 9, 10, and 11 plot the integral response of voltage shift for three devices. There is considerable variation between the different manufactures. This effect will be investigated to increase sensitivity to microdose of future dosimeters.

Fig. 9 shows the results of the Toshiba parts. Results from nickel and iodine exposures are shown in Figures 9a and 9b, respectively. The Toshiba parts exhibit a narrow pre-irradiation shift distribution. This property makes the device a sensitive micro-dosimeter, since the number of false positives will be small. Fig. 9b shows the onset of shifts at 1 volt increments. This effect is an artifact of the measurement technique. The protocol used for iodine underestimated the response to these high LET ions. Fig. 9c shows the number of shifts as a function of fluence. The data is fit to linear model and the slope, which is the effective cross section of the shifts, depends on the LET. There is considerable spread in the data, which is most likely due to part-to-part variation. The slope of the linear response is the effective cross section of the device. The slope is 9.91E-6 cm^2 for nickel and 1.35E-5 cm^2 for iodine. The SEU cross section for these types of devices is approximately 1E-2 cm^2 for nickel and iodine. This disagreement implies that different mechanisms and sensitive volumes are responsible for SEU and SHE events.

Fig. 10 shows the results of the ISS parts. Nickel and iodine are shown in Figures 10a and 10b, respectively. Fig. 10c shows the number of shifts as a function of fluence. The magnitude of the threshold shifts and number of events is invariant to LET. The effect could have saturated at the LETs used in this experiment. The data is modeled on a power law. The ISS parts exhibit wide pre-irradiation shift distributions, but the microdose effect is very pronounced. Threshold shifts occur well outside of the control distribution.

Fig. 11 shows the results of the IDT parts. Nickel and iodine are shown in Figures 11a and 11b, respectively. The equal steps of largest shifts in Fig. 11b are an artifact of the measurement technique. The experimental protocol for this run underestimated the shift that iodine would induce. Certain bits, therefore, show events at the highest measured voltage. Fig. 11c shows the number of shifts as a function of

fluence. The number of shifts increases with fluence, but not in a measurable way.

V. Discussion

The testing of SRAMs for dosimetry applications has yielded several findings. The foremost is that the response of the device to total dose within the operational dynamic range of the device is negligible. This fact agrees with the hypothesis that equal exposure to all four of the SRAM transistors will not change the cell's threshold error voltage. It is also possible that the SRAM cells are insensitive to radiation under the 20 krad limit set in this study. This response disagrees with the heavy ion data, where some cells show a large error voltage increase with low total dose to one cell. A single ion hit can result in a wide range of equivalent doses to a sensitive volume, from less than one krad to several tens of krads, depending on the circumstances.

The second major result is the response of individual cells to radiation. Three of the four tested devices show strong dependence of error voltage shift on fluence and LET. Two trends in the response of the device to heavy ions were observed, both of which are important to microdose measurement techniques. All devices demonstrated a monotonic increase with ion fluence of the total number of error shifts greater than 0.01V. Considering the small percentage of cells affected, the events are mostly caused by single hits to the gate oxides. The dependence of the number of events on the LET is complex. Two part types exhibit increase in the number of events with increased LET, while two part types show negligible change. This variance will provide important information in determining the most sensitive parameters of the SRAM cell.

Finally, while each part shows a repeatable response, the variation between manufacturers stands out as an important variable to gauge sensitivity of each part to radiation. The Cypress part showed very little response on the micro or macro scale. The other parts demonstrated the same trend of fluence and LET dependence, but with widely varying sensitivities. Visual inspection of the devices shows obvious differences in the layout of the cells and the peripheral circuitry on the die. This implies that there are differences in sense amps and SRAM cell layout, which would necessarily introduce variation in the microdose response.

The application would be a microdosimeter that is not affected by a continuous total dose radiation field. This application is contrast to other array dosimeters, e.g., dosimeters based on DRAMs or PROMs, which exhibit an aggregate effect as well as a microdose effect. The device could be employed in a mixed radiation field that would report large and rare energy depositions without the non-struck cells reporting any accrued dose. Current research does not provide sufficient information concerning the development of a method to differentiate between ion hits. This effect will be addressed in later studies.

An additional application for this phenomenon is a method to monitor the integrity of the gate oxides in a heavy ion environment. Further research is underway to correlate SRAM cell response to heavy ion radiation. This method will allow a general method of measuring gate oxide degradation. Another application available for these devices with no modification or further research is the identification of latent SHE by reading a device at reduced bias. A flight board would be designed reduce operating bias to scan for latent SHE.

VI. Conclusions

Ionizing radiation changes the lowest operating bias at which the device can be readout for heavy ions but not for overall total dose. The TID radiation robustness appears to be due to the symmetry of the SRAM cell yielding less sensitivity. Reading the data does not destroy or alter the data, nor does it prevent continued measurement with the same device. Manufacturing variance is an important factor in the determination of the sensitivity of the part. Since these parts vary greatly, examining the difference in their manufacture should yield data on their sensitivity. Work is ongoing to increase the sensitivity in order to be useful for oxide monitoring. Techniques are also being developed to extend the range of these dosimeters for longer measurement cycles and extremely harsh environments.

References

[1] T. P. Ma and P.V. Dressendorfer, Ionizing Radiation Effects in MOS Devices and Circuits, New York: John Wiley and Sons, 1989.

[2] A. B. Rosenfeld, et al., *IEEE Trans. on Nucl. Sci.*, vol. 43, no. 6, pp. 2693 –2700, Dec. 1996.

[3] A. B. Rosenfeld, et al., *IEEE Trans. on Nucl. Sci.*, vol. 46, no. 6, pp. 1774 –1780, Dec. 1999.

[4] J. Barak, et al., *IEEE Trans. on Nucl. Sci.*, vol. 46, no. 6, pp. 1342 -1353, Dec. 1999.

[5] D. R. Roth, P. J. McNulty, W. G. Abdel-Kader, L. Strauss, E.G. Stassinopoulos, *IEEE Trans. on Nucl. Sci.*, vol. 40, no. 6, pp. 1721 –1724, Dec. 1993.

[6] C. S. Yue, J. Kueng, P. Fechner, T. Randazzo, *SOS/SOI Technology Conference*, 1990, IEEE, pp. 173 –174, 1990 .

[7] K. Hirose, et al., *Radiation Effects Data Workshop*, IEEE, pp. 48 –50, 2001.

[8] J. P. David, J. G. Loquet, S. Duzellier, *Radiation and Its Effects on Components and Systems*, 1999. RADECS 99. 1999 Fifth European Conference on, pp. 80 –86, 2000.

[9] M. R. Shaneyfelt, et al., *IEEE Trans. on Nucl. Sci.*, vol. 44, no. 6, pp. 2040 –2047, Dec. 1997.

[10] B. Doucin, et al., *Radiation and Its Effects on Components and Systems*, RADECS 97, Fourth European Conference on, pp. 561 –569, 1998.

[11] J. M. Benedetto, A. Jordan, N. LaValley, *Radiation Effects Data Workshop*, pp. 16 –20, 2000.

[12] C. Poivey, T. Carriere, J. Beaucour, T. R. Oldham, *IEEE Trans. on Nucl. Sci.*, vol. 41, no. 6, pp. 2235 –2239, Dec. 1994.

[13] O. Calvo et al., *Integrated Circuit Design*, Proceedings from XI Brazilian Symposium on, pp. 78 –81, 1998.

[14] A. I. Chumakov, A. V. Yanenko, *IEEE Trans. on Nucl. Sci.*, vol. 43, no. 6, pp. 3109 –3114, Dec. 1996.

[15] P.E. Dodd, et al., *IEEE Trans. on Nucl. Sci.*, vol. 48, no. 6, pp. 1893 –1903, Dec. 2001.

[16] G. Cellereet al., *IEEE Trans. on Nucl. Sci.*, vol. 48, no. 6 Part: 1, pp. 2222 –2228, Dec. 2001.

[17] L. Z. Scheick, S. M. Guertin, G. M. Swift, *IEEE Trans. on Nucl. Sci.*, vol. 47, no. 6, pp. 2534 –2538, Dec. 2000.

[18] L. Z. Scheick, P. J. McNulty, D. R. Roth, M. G. Davis, B. E. Mason, *IEEE Trans. on Nucl. Sci.*, vol. 46, no. 6, pp. 1751 –1756, Dec. 1999.

[19] H. Kuriyama, et al., *IEEE Trans. on Electronic Devices.*, vol. 46, no. 5 , pp. 927 –932, May 1999.